



Effect of electrolysis parameters on the morphologies of copper powders obtained at high current densities

GÖKHAN ORHAN* and GİZEM GÜZEY GEZGIN

Istanbul University, Faculty of Engineering, Metallurgical and Materials
Engineering Department, 34320 Istanbul, Turkey

(Received 27 June, revised 20 October 2011)

Abstract: The effects of copper ion concentrations and electrolyte temperature on the morphologies and on the apparent densities of electrolytic copper powders deposited at high current densities under galvanostatic control were examined. These parameters were evaluated by the current efficiency of hydrogen evolution. In addition, scanning electron microscopy was employed for analyzing the morphology of the copper powders. It was found that the morphology was dependent on the copper ion concentration and electrolyte temperature under same current density (CD) conditions. At 150 mA cm⁻² and a potential of 1000±20 mV (vs. SCE), porous and disperse copper powders were obtained at low concentrations of Cu ions (0.120 M Cu²⁺ in 0.50 M H₂SO₄). Under these conditions, a high rate of hydrogen evolution occurred parallel to copper electrodeposition. The morphology was changed from porous, disperse and cauliflower-like to coral-like, shrub-like and stalk-stock-like morphology with increasing Cu ion concentrations from 0.120, through 0.155, 0.315 and 0.475 to 0.630 M Cu²⁺ in 0.5 M H₂SO₄, respectively, at the same CD. Similarly, with increasing temperature, the powder morphology and the apparent density changed. The apparent density values of the copper powders were suitable for many powder metallurgy applications.

Keywords: electrolytic copper powder; apparent density; hydrogen evolution; scanning electron microscopy (SEM).

INTRODUCTION

Copper powder is widely used in electronics and powder metallurgy and it can be produced by a number of methods. There are four main commercially available methods: electrochemical, reduction of copper oxide, chemical precipitation and atomization. The shape, size and other physical properties of copper powders strongly depend on the manufacturing technique.¹⁻³

*Corresponding author. E-mail: gorhan@istanbul.edu.tr
doi: 10.2298/JSC110627196O

Electrolysis is an economic processing method that requires low capital investment, energy consumption and operational costs. Since this method enables the production of metal powder of high purity, it has the advantages of good green strength and low oxygen content compared to the other alternative powder production technologies. Another significant feature of this method is that it allows for the production of powders with a wide range of apparent densities ($0.4\text{--}4.0\text{ g cm}^{-3}$).⁴

An electrolytic metal powder represents disperse electrodeposits removed from the electrode by tapping or some other similar manner. In potentiostatic systems, disperse copper deposits are obtained at overpotentials on the plateau of the limiting current density, as well as at higher ones (at the end of this plateau). The copper electrodeposition process occurs simultaneously with the hydrogen evolution reaction. In galvanostatic systems, electrodeposition of copper has the tendency to form powders when current densities larger than the limiting diffusion current density are used (or overpotentials outside the plateau of the limiting diffusion current density).^{2,5–8} In addition, increasing the overpotential or current density leads to the formation of more dispersed deposits characterized by decreased particle size. The only real difference lies in the morphology of the powder particles obtained by potentiostatic and galvanostatic deposition, *i.e.*, particles obtained by galvanostatic deposition are less dendritic than those obtained by potentiostatic deposition, because the overpotential at the end of the deposition is less negative than in the latter case.⁶

The most important properties of a metal powder are its specific surface area, apparent density, flowability and particle grain size and distribution.⁵ These properties, which are typically known as decisive properties, characterize the behavior of a metal powder. The morphologies of copper powder particles correlated with the apparent density and flowability have been reported by Pavlović *et al.*⁹ and Popov *et al.*^{10,11} It can be seen from these investigations that the more dendritic is the structure of the powder particles, the lower is the apparent density of the copper powder. Popov *et al.*¹⁰ also proposed a method for the determination of the critical apparent density which permits the free flow of electrodeposited copper powders. The apparent density or volumetric mass is defined as the mass per unit volume and can also be determined experimentally. The powder particles from the same fraction of different powders occupy approximately the same volume, but, depending on the structure of the metallic copper, exhibit different apparent densities.

Many investigators studied the electrodeposition of copper deposits from acidic sulfate solutions by potentiostatic or galvanostatic methods. The morphologies of copper deposits obtained at overpotentials belonging to the plateau of the diffusion limiting current density and larger overpotentials were investigated. The results showed that the morphologies and the properties of the copper de-

posites were strongly dependent on parameters such as overpotential, quantity of evolved hydrogen,^{5,7,8} current density,^{3,12,13} concentrations of copper ions^{3,14} and H₂SO₄^{15,16} and temperature of the solution.^{3,17}

The aim of this study was to produce copper powders from acid sulfate solutions by means of electrolysis using a conventional electrolysis cell with scraper that provides faster ionic movement due to the convective diffusion at the electrode–electrolyte interface. The morphologies of the copper powders and their apparent densities were investigated as a function of current density, copper ion concentration and temperature of the electrolyte.

EXPERIMENTAL

Electrodeposition of the copper powders onto vertical flat cathode with a scraper was performed in a laboratory-scale electrolysis cell. A stainless steel cathode with an area of 30 cm² (2 cm×15 cm) and two lead anodes were used. The surface of the cathodes was ground and polished prior to each experiment. The total electrolyte volume was 3.5 dm³. One of the most important technological problems faced in electrolysis is the continuity of the process due to changes in the size of the cathode. In the designed cell, the metal powder produced is removed from the cathode surface by two scrapers, which leads to the accumulation of the powder at the bottom of the cell. Thus, the cathode size is kept constant and the problem of the continuous increasing of cathode surface area is solved. It is important to note that the cathode-scraper was positioned at a distance of 1 mm from the surface of the cathode and a scraper speed of 10 cycles per min was used in all the experiments.

Doubly distilled water and analytical grade chemicals were used for the preparation of the solution for the electrodeposition of copper. The electrolyte circulation rate was kept constant at 1.0 dm³ min⁻¹. In the experiments, electrolytic copper powder was galvanostatically deposited from the following solutions:

- a) 0.120 M Cu²⁺ (solution I),
- b) 0.155 M Cu²⁺ (solution II),
- c) 0.315 M Cu²⁺ (solution III),
- d) 0.475 M Cu²⁺ (solution IV) and
- e) 0.630 M Cu²⁺ (solution V),

all in 0.5 M H₂SO₄.

Following the electrolysis, the obtained powder was washed several times with distilled water. Then, in order to prevent oxidation, the powder was rinsed with ethanol and dried at 95 °C in a drying train under vacuum. The current density *vs.* voltage curve was measured using linear sweep voltammetry (Gamry Instrument PCA 750). For the majority of the experiments, the potential was swept from 0 to -1200 mV *vs.* standard calomel electrode (SCE). All the potentials in the paper are given with respect to SCE. The employed scan rate was 0.5 mV s⁻¹.

The powder particles were characterized using a scanning electron microscope (JEOL JSM 5600). The concentration of copper ions in the electrolyte before and after the electrodeposition was measured by inductively coupled plasma atomic emission spectroscopy (ICP). Using these data and the Faraday Law, the current efficiencies of the copper electrodepositions were determined. Assuming that the only electrochemical processes on the cathode were Cu deposition and H₂ evolution and ignoring current losses, the hydrogen evolution efficiency was calculated. The apparent densities of copper powder were measured by a 2 cm³ minimized Arnold meter.



RESULTS AND DISCUSSION

The polarization curves for copper electrodeposition from solutions I, III and V are shown in Fig. 1, from which it can be seen that the beginning of the plateau of the limiting diffusion current density was rapidly shifted to lower electrodeposition potentials with decreasing concentration of Cu ions. The range of potentials belonging to the plateau of the limiting diffusion current density for solutions I, III and V were 140–840 mV, 240–900 mV and 380–1020 mV, respectively. It is known that the hydrogen evolution reaction accompanies copper electrodeposition at high overpotentials and the significant hydrogen evolution occurred at the cathode surface at the potentials more negative than –840, –900 and –1020 mV for solutions I, III and V, respectively.

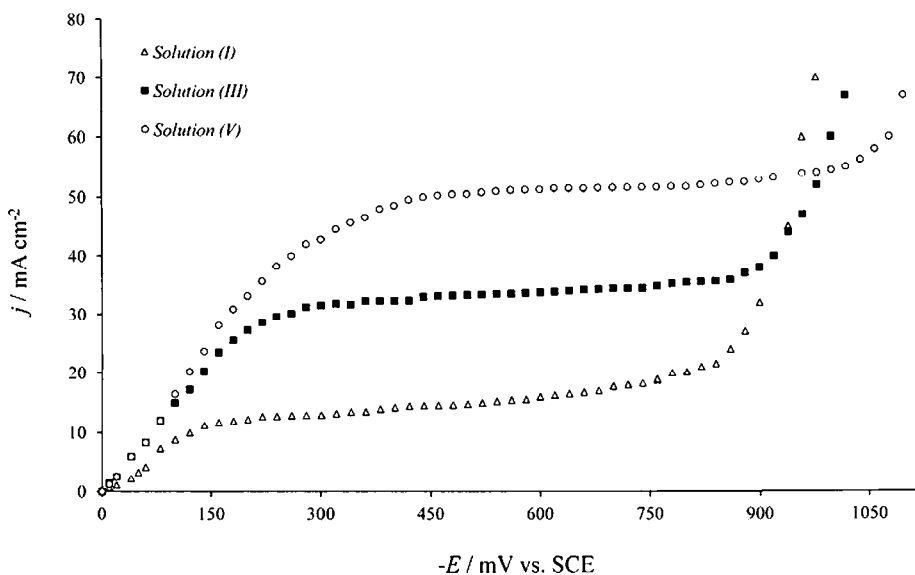


Fig. 1. Polarization curves for the cathodic process of copper deposition from solutions I, III and V.

The cathode polarization *vs.* time curves, which were obtained by repeated experiments run under galvanostatic conditions, are displayed in Fig. 2. The cathode potential on the electrode surface shifted towards more negative values with decreasing Cu ions concentrations in the electrolyte. On the other hand, during the electrodeposition process, the potential values fluctuated with the amplitude by approximately ±20 mV. Since the cathode surface was scraped at a distance of approximately 1 mm from its surface, the dendrite lengths and the related surface area remained relatively constant, and thus the potential curves can be considered to have a smooth character. At a CD of 150 mA cm⁻², the

potential values were approximately 1000, 700, 600 and 400 mV for solutions I and III–V, respectively.

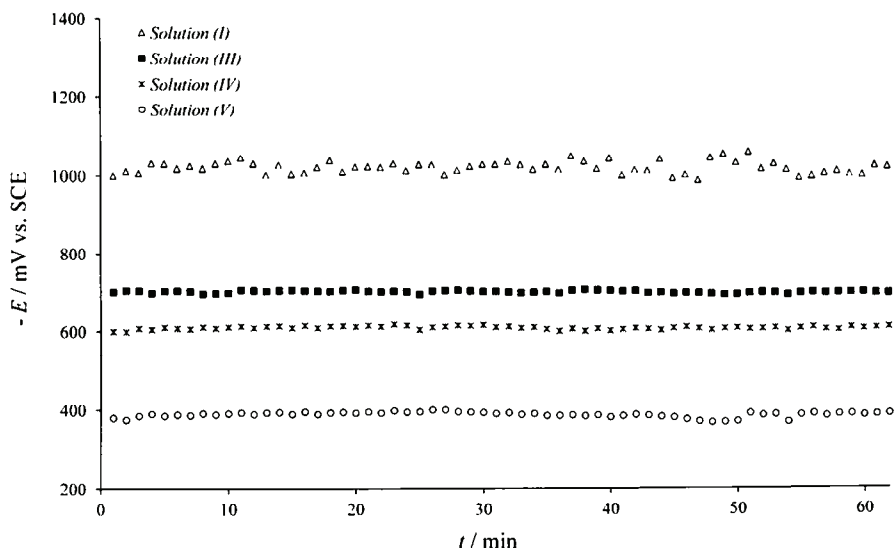


Fig. 2. Cathodic polarization value *vs.* time of copper deposition from solutions I and III–V.

The effect of current density on the morphology of electrolytic copper powder and on the properties of the copper powder was investigated at CD values of 150 and 200 mA cm⁻² and with different Cu ions concentrations at 30 °C.

The results obtained from solution I are shown in Fig. 3. Figures 3a and 3b show the morphologies of the copper powder obtained at 150 mA cm⁻². From Fig. 3a, it can be seen that a very disperse structure was formed at a CD of 150 mA cm⁻². The formed particles consisted of small cauliflower-like agglomerates of copper grains (Fig. 3b). Similar morphologies of the powder particles were obtained at a CD of 200 mA cm⁻² (Figs. 3c and 3d), which can be explained by the fact that both particles were formed under conditions of vigorous hydrogen evolution. It can be concluded that both types of powder particles consisted of agglomerates of copper grains. The only difference lay in the size of the individual copper grains of which these agglomerates were constituted. The estimated average size of copper grains in Fig. 3b is about 850±100 nm while it is about 400±100 nm in Fig. 3d. The nucleation rate and the grain size depend on the CD; thus, the grain size is considerably decreased at 200 mA cm⁻². According to Popov,⁶ the deposits obtained at low CDs grew from a small number of nuclei. However, with the increasing CD, the number of growth sites increased and the grain size of the deposit decreased. This is in good agreement with the fact that particles obtained at the low CD (Figs. 3a and 3b) were less branched and denser than those obtained at the higher CD (Figs. 3c and 3d). The increase of dispersity

and the decrease in grain size are the result of both the increased nucleation rate and the intensification of the hydrogen evolution reaction with increasing CD.

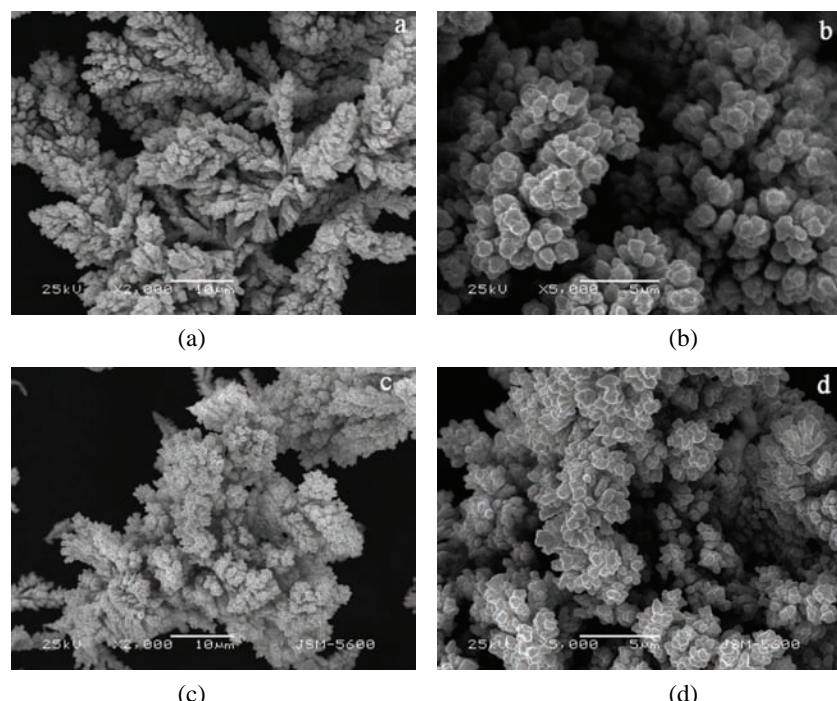


Fig. 3. SEM Photomicrographs of copper powder particles obtained from solution I at current densities of: 150 (a and b) and 200 mA cm^{-2} (c and d).

The morphologies of copper powders obtained from solution II at CDs of 150 and 200 mA cm^{-2} are shown in Fig. 4. From Figs. 4a and 4c, it may be seen that the powder particles were coral-like and consisted of small cauliflower-like agglomerates of copper grains. On the other hand, it can be said that the aggregated copper particles were globular at the high CD (Fig. 4d). The one directional growth of the powder particles can be clearly seen in Fig. 4.

As can be seen from Fig. 5, the copper powder particles obtained from solution III at both current density values had a denser deposit structure and consisted of aggregated copper grains. At higher magnifications, it can be easily seen that the shape of these grains could be characterized as globular (Figs. 5b and 5d). The copper deposit obtained from this solution at both CDs had a cauliflower-like structure. However, the size of the cauliflower-like particles increased with increasing copper ion concentration. Furthermore, the tendency of single directional growth can be clearly seen, which is similar to the deposits obtained from solution II.

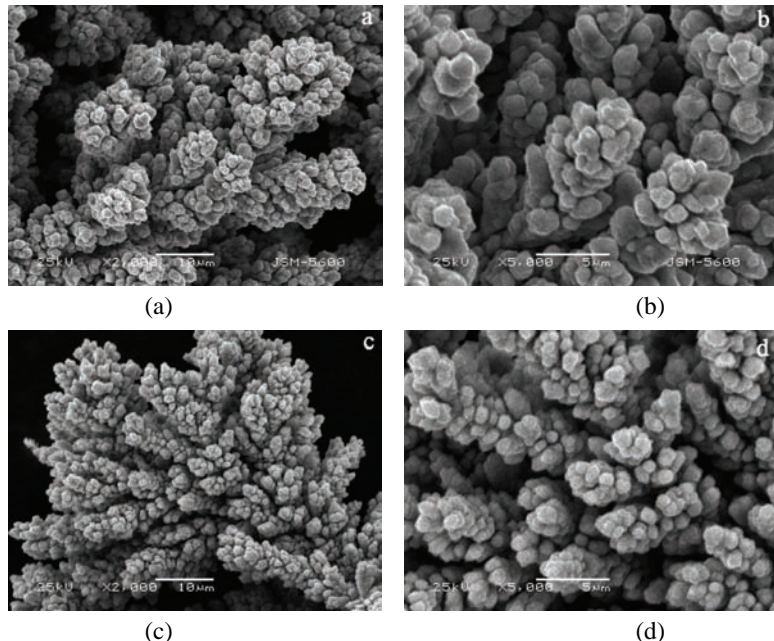


Fig. 4. SEM Photomicrographs of copper powder particles obtained from solution II at current densities of: 150 (a and b) and 200 mA cm⁻² (c and d).

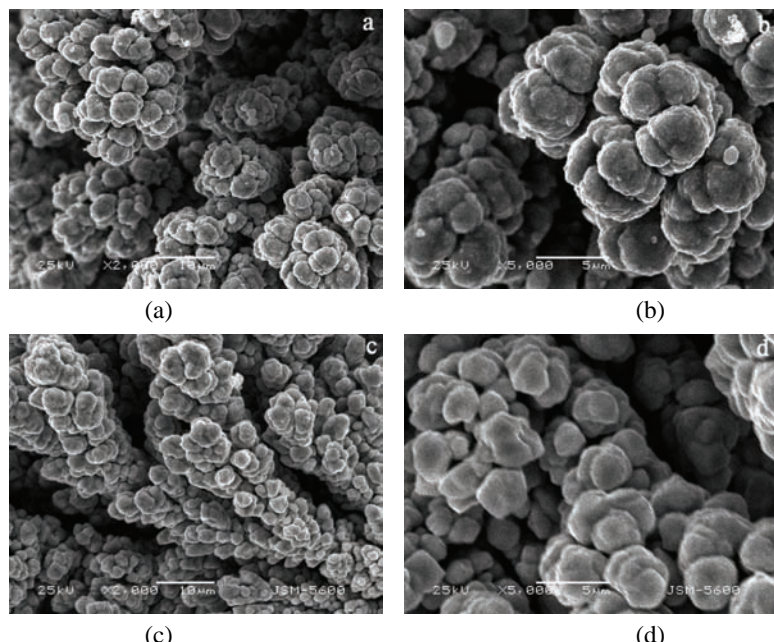


Fig. 5. SEM Photomicrographs of copper powder particles obtained from solution III at current densities of: 150 (a and b) and 200 mA cm⁻² (c and d).

The shrub-like morphology of the copper obtained from Solution IV at CDs of 150 and 200 mA cm⁻² can be seen in Fig. 6. This structure consisted of bunched copper grains (Fig. 6a). Copper powder morphology and size at both CDs from this electrolyte are the same. It can be concluded that the upper surface of this structure has porous character (Fig. 6b). It is important to note that the bunches were observed at higher magnifications.

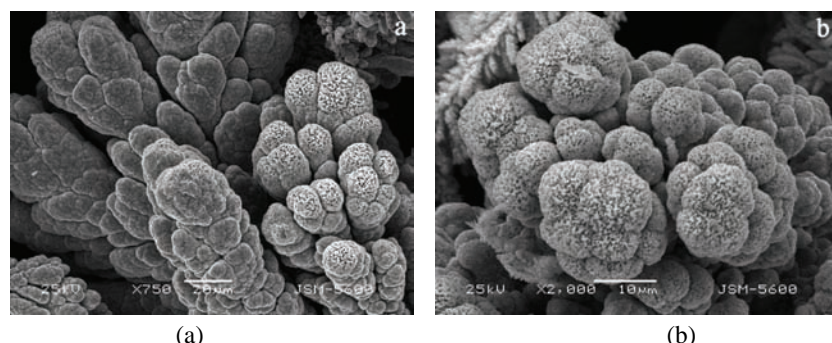


Fig. 6. SEM Photomicrographs of copper powder particles obtained from solution IV at current densities of: 150 (a) and 200 mA cm⁻² (b).

It can be seen from Fig. 7 that a denser deposit of the copper powder particles was obtained from solution V at 150 mA cm⁻², which consisted of aggregated copper grains. The shape of these grains can be characterized as coarse.

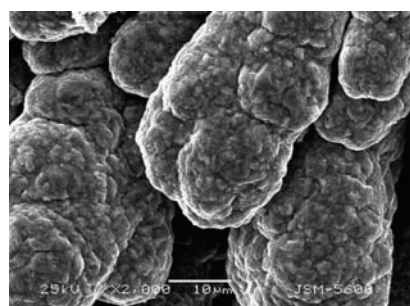


Fig. 7. SEM Photomicrograph of copper powder particles obtained from solution V at 150 mA cm⁻².

The average current efficiencies for the hydrogen evolution reaction at 30 °C for various CDs and Cu concentrations are given in Table I. It can be seen that hydrogen evolution efficiency decreased with increasing Cu ion concentration and increased with increasing CD. The current efficiency of hydrogen evolution obtained from solution I at 150 mA cm⁻² was 24.4 %, while it was 28.6 % at 200 mA cm⁻². This value decreased with the increasing Cu ion concentration at both CDs and became zero for solution V. The current efficiency value of zero for hydrogen evolution indicates that all the current in the system was consumed for copper electrodeposition. Thus, according to Nikolić,^{7,10} an average current effi-

ciency of hydrogen evolution of 30 % is sufficient to cause mixing of the solution in the near-electrode layer while simultaneously decreasing the diffusion layer thickness and increasing the limiting diffusion current density. Due to the change in the hydrodynamic conditions caused by vigorous hydrogen evolution, the morphologies of the deposits become similar to those obtained at some lower overpotential, before the initiation of dendritic growth.⁵ This clearly explains the cauliflower-like shape of the powders obtained in this work.

TABLE I. The values of the average current efficiencies of hydrogen evolution, in dependence on the copper ion concentration and current density

Cu^{2+} concentration, mol dm^{-3}	Hydrogen evolution efficiency, %	
	150 mA cm^{-2}	200 mA cm^{-2}
0.120	24.4	28.6
0.155	12.5	13.2
0.315	3.8	4.5
0.475	0.6	0.8
0.630	0	0

The copper ion concentration and the CD are significantly important parameters determining the limiting current density; thus, they determine the morphology and size of electrolytic copper powders. According to Levich, in metal electrodeposition under natural convection, the limiting current density (i_L) varies with concentration as:¹⁴

$$i_L \approx c_0^{1.25} \quad (1)$$

where c_0 is concentration of Cu ions.

According to Eq. (1), the limiting current density increases with the increasing concentration of Cu ions. Finally, with increasing limiting current density, the morphologies of copper powder at higher copper ion concentrations were similar to those obtained at lower CDs, despite working at a higher CD. In other words, when the copper concentrations are high, the working CD actually stays below the limiting diffusion current density.

The change in the morphologies of the electrolytic copper powder with concentration of copper ions in solution under galvanostatic control can be seen in Figs. 3a, 4a, 5a, 6a and 7 for a CD of 150 mA cm^{-2} or in Figs. 3c, 4c, 5c and 6c for a CD of 200 mA cm^{-2} . The morphologies changed to cauliflower-like, coral-like, shrub-like, and stalk-stock-like morphology with increasing of Cu ion concentrations from 0.120, through 0.15, 0.315 and 0.475, to 0.630 M Cu^{2+} in 0.5 M H_2SO_4 , respectively, at the same CD. The particle size variation depending on the applied CD was in good agreement with the nucleation rate and nuclei growth rate. With increasing CD, the grain size will be finer and may lead to an increase in the dispersity of copper deposits, because the nucleation rate is greater than nuclei growth rate.^{3,5,7,18}

The apparent densities for the copper powder obtained at 150 and 200 mA cm⁻² for various copper concentrations under standard conditions are given in Table II, from which it can be seen that the properties of the powder changed with the applied CD. This can be explained as follows: the decrease in the size of the grains with increasing of CD or with decreasing Cu ion concentrations leads to an increase in the specific surface area of the powder. It is known that an increase in the specific surface area of a powder results in a decrease in the apparent density.^{3,5,9,11} As can be seen in Table II, the obtained results are in accordance with the surface area-apparent density relation. While the apparent density values varied from 0.68 to 3.38 g cm⁻³ with increasing Cu ion concentration at 150 mA cm⁻², the apparent density varied between 0.58–3.43 g cm⁻³ at a CD of 200 mA cm⁻².

TABLE II. Apparent density of the copper powder obtained at different CDs and Cu concentrations at 30 °C

Cu ²⁺ concentration, mol dm ⁻³	Apparent density, g cm ⁻³	
	150 mA cm ⁻²	200 mA cm ⁻²
0.120	0.68	0.58
0.155	0.88	0.66
0.315	1.11	1.62
0.475	3.10	2.57
0.630	3.38	3.43

To understand the effect of electrolyte temperature on the Cu powder morphology and apparent density, the powders obtained from solution II were investigated. The morphologies of electrolytic copper powder particulates obtained from solution II at a CD of 150 mA cm⁻² at 45 and 60 °C are shown in Fig. 8. It can be stated that powder particles obtained at all three temperatures (30, 45 and 60 °C) were branched structures and the branches consisted of agglomerated copper grains (Figs. 4a, 8a and 8c). The variation of the morphology with increasing temperature can be clearly observed at higher magnifications. The surface properties of the powders obtained at 45 and 60 °C differ from the velvety structure of the powder obtained at 30 °C. It is well known that an increase in the specific surface area of a powder means a decrease in the apparent density. The apparent densities of powders obtained at an electrolyte temperature of 30, 45 and 60 °C were 0.88, 0.65, and 0.38 g cm⁻³, respectively. As expected, a decrease in the apparent density with increasing surface area was observed. The morphology of copper powder particles obtained at 200 mA cm⁻² CD from solution II at 60 °C is shown in Fig. 9. It can be seen from 30 (Figs. 4c and 4d) and 60 °C (Fig. 9) that the powder particles are sponge-like. It can also be seen that copper particles have globular structure.

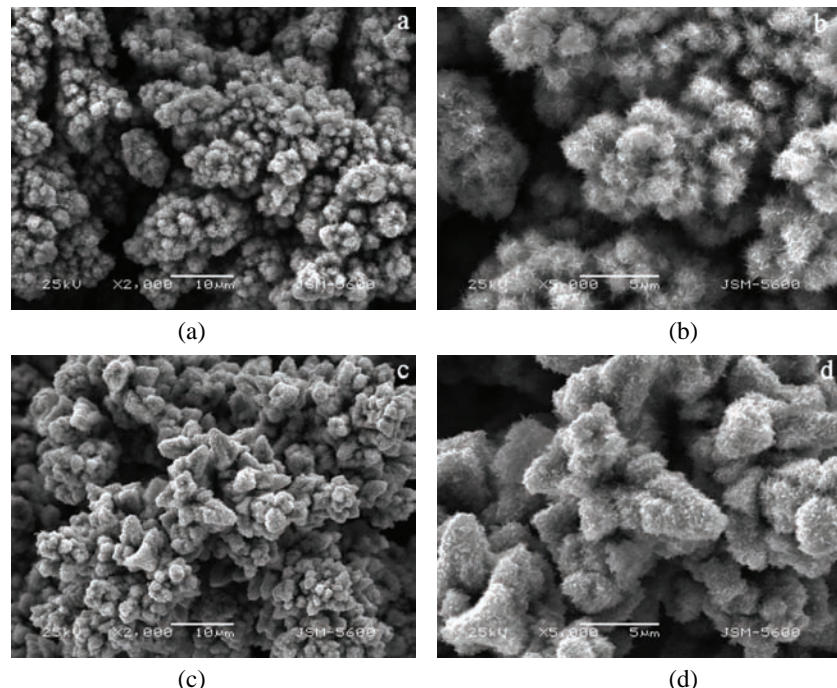


Fig. 8. SEM Photomicrographs of copper powder particles obtained from solution II at temperatures of: 45 (a and b) and 60 °C (c and d) at 150 mA cm^{-2} .

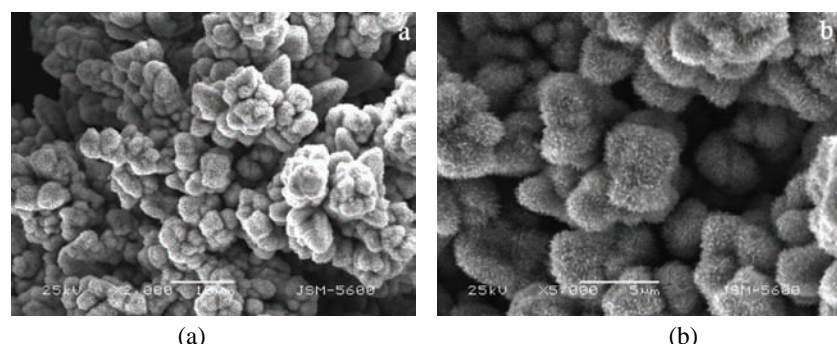


Fig. 9. SEM Photomicrographs of copper powder particles obtained from solution II at a temperature of 60 °C at 200 mA cm^{-2} .

The powder obtained at 200 mA cm^{-2} from solution II and at 60 °C is had the same velvety structure as the powder obtained at 150 mA cm^{-2} and at 45 and 60 °C. The apparent density values of the powders obtained at 30 and 60 °C under the same experimental conditions were 0.66 and 0.42 g cm^{-3} , respectively. These are in good agreement with the morphologies of the respective copper powders.

In the experiments in which the electrolyte temperature was 30 °C, the average current efficiency of the hydrogen evolution was 12.5 % in solution II at a CD of 150 mA cm⁻², while at 45 and 60 °C, the average current efficiencies of hydrogen evolution were 25.5 and 38.2 %, respectively. On the other hand, the average current efficiency of hydrogen evolution in solution II at a CD of 200 mA cm⁻² and at 30 °C was 13.2 %. When the temperature was increased to 60 °C, the average current efficiency of hydrogen evolution increased to 41.1 % in the same solution.

All powders that were obtained from solutions I–III at a CD of 150 or 200 mA cm⁻² and at temperatures 30–60 °C consisted of agglomerates of copper grains. The size of the grains in these agglomerates was a function of the CD (*i.e.*, of the overpotential), Cu ion concentration, temperature and quantity of evolved hydrogen. The decrease in the mean size of the grains was related to the increasing quantity of evolved hydrogen.

SEM Images of powders obtained in the absence of the scrapper are shown in Fig. 10. In this case, the surface area of the electrode continues to enlarge, which leads to a decreasing current density. The powder obtained under these conditions does not have a homogenous structure. The powder structure was comprised of agglomerated copper grains, which grew extremely like the cauliflower-like grains (Fig. 10a). These powders seem to be a mixture of powders with different grain structures because of the surface, which could not remain constant due to the absence of the scrapper. The denser-like deposit structure obtained from solutions IV and V as seen in Part A and the cauliflower-like structure obtained from solution II as seen in Part B of Fig. 10b simultaneously co-existed.

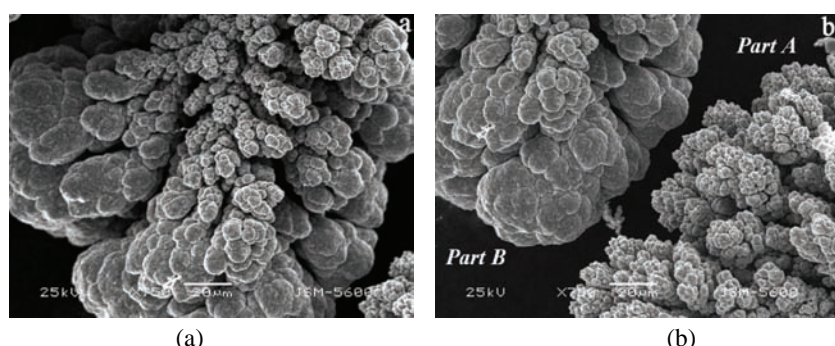


Fig. 10. SEM Photomicrographs of copper powder particles obtained from solution II at 150 mA cm⁻² without a scraper.

CONCLUSION

The effect of different Cu ion concentrations, temperature and current density on the morphology and apparent density of copper powders obtained at high

CDs were examined. The concentration of H_2SO_4 and the scraper speed were kept constant. The following conclusions may be deduced.

The morphologies of the disperse and porous copper powders from solutions I and II were small cauliflower-like agglomerates of copper grains at current density values of 150 and 200 mA cm^{-2} . It is important to note that the powders from solution II were denser than those from solution I. Thus, this structure can be called coral-like. The particles from solution III were also in cauliflower-like form at CDs values of 150 and 200 mA cm^{-2} . In solution IV, the particles were shrub-like in form at both applied CDs and finally a stalk-stock-like form were found in solution V at a CD of 150 mA cm^{-2} under the same working conditions. The morphologies of the copper powder obtained at the applied CDs, *i.e.*, overpotentials, were in accordance with the position of the CD on the polarization curve. In other words, the morphologies of the copper powders were correlated with the hydrogen evolution rates. The cauliflower-like structure was the main characteristic of deposits obtained at high CDs and high overpotentials, belonging to the limiting diffusion current density plateau, at which the hydrogen evolution rate was high. However, when the hydrogen evolution rate was lower, the morphologies changed from small cauliflower-like agglomerates of copper grains to sponge-like, shrub-like or stalk-stock-like shape.

Temperature also has a significant influence on the copper powder morphology along with current density and copper ion concentration. The velvety structure of the powders obtained at 45 and 60 °C, which is different to that formed at 30 °C, is noteworthy. This structure resulted in an increase in the surface area and, consequently, a decreased apparent density.

The apparent density values of the copper powder also changed with respect to their morphologies. The smaller the cauliflower-like structure of the powder particulates, the lower was the apparent density of the copper powder. Therefore, the apparent densities of copper powders can be controlled by changing the electrolysis parameters. Depending on the electrolysis parameters, such as CD, Cu ion concentration and temperature, the apparent densities of copper powders were within the range 0.38 and 3.43 g cm^{-3} .

Moreover, the importance of the employment of a scrapper is dominantly seen in this work. It allows for a homogenous powder production. In addition, pre-determined particles of copper-plated electrodes can be obtained on the surface.

Acknowledgement. The authors would like to thank the Scientific and Technological Research Council of Turkey (TUBITAK), which supported this work as part of the TUBITAK Project No. 105M137.

И З В О Д

ЕФЕКТИ ПАРАМЕТАРА ЕЛЕКТРОЛИЗЕ НА МОРФОЛОГИЈУ БАКАРНОГ ПРАХА
ДОБИЈЕНОГ ПРИ ВИСОКИМ ГУСТИНАМА СТРУЈЕ

GÖKHAN ORHAN и GİZEM GÜZEY GEZGIN

*Istanbul University, Faculty of Engineering, Metallurgical and Materials Engineering
Department, 34320 Istanbul, Turkey*

Испитиван је утицај концентрације јона бакра и температуре електролита на морфологију и привидну густину бакарног праха добијеног у галваностатском режиму при високим густинама струје. Ови параметри су одређени искоришћењем струје издавања водоника при таложењу бакра. Поред тога, морфологија бакарног праха је анализирана и скенирајућом електронском микроскопијом. Нађено је да морфологија прахова добијених при истој густини струје зависи од концентрације јона бакра у електролиту и температуре електролита. Таложењем при густини струје 150 mA cm^{-2} и потенцијалу $-1000 \pm 20 \text{ mV}$ (према ЗКЕ) из електролита који је садржао $0,120 \text{ M Cu}^{2+}$ и $0,50 \text{ M H}_2\text{SO}_4$ добијен је порозан и дисперзан прах бакра. Под тим условима паралелено са таложењем бакра интензивно се издаваја водоник. Са повећањем концентрације јона Cu^{2+} од $0,120, 0,155, 0,315, 0,475$ до $0,630 \text{ M}$ при истој густини струје, запажена је промена морфологије праха од порозне, дисперзне и облика сличних карфиолу до морфологије која подсећа на корале, жбунове и стабљике. Повећање температуре такође утиче на морфологију и привидну густину бакарног праха. Вредности привидне густине прахова таложених током овог испитивања показују да су они погодни за примену у разним областима металургије.

(Примљено 27. јуна, ревидирано 20. октобра 2011)

REFERENCES

1. A. Agrawal, S. Kumari, D. Bagchi, V. Kumar, B. D. Pandey, *Hydrometallurgy* **84** (2006) 218
2. M. G. Pavlović, K. I. Popov, <http://electrochem.cwru.edu/encycl/art-p04-metalpowder.htm>, 2005
3. G. Orhan, G. Hapçı, *Powder Technol.* **201** (2010) 57
4. M. G. Pavlović, Lj. J. Pavlović, I. D. Doroslovački, N. D. Nikolić, *Hydrometallurgy* **73** (2004) 155
5. N. D. Nikolić, Lj. J. Pavlović, M. G. Pavlović, K. I. Popov, *Powder Technol.* **185** (2008) 195
6. K. I. Popov, S. S. Djokić, B. N. Grgur, *Fundamental Aspects of Electrometallurgy*, Kluwer Academic/Plenum Publishers, New York, USA, 2002
7. N. D. Nikolić, K. I. Popov, Lj. J. Pavlović, M. G. Pavlović, *Surf. Coat. Technol.* **201** (2006) 560
8. N. D. Nikolić, K. I. Popov, Lj. J. Pavlović, M. G. Pavlović, *J. Electroanal. Chem.* **588** (2006) 88
9. M. G. Pavlović, Lj. J. Pavlović, E. R. Ivanović, V. Radmilović, K. I. Popov, *J. Serb. Chem. Soc.* **66** (2001) 923
10. K. I. Popov, S. B. Krstić, M. G. Pavlović, *J. Serb. Chem. Soc.* **68** (2003) 511
11. K. I. Popov, S. B. Krstić, M. C. Obradović, M. G. Pavlović, Lj. J. Pavlović, E. R. Ivanović, *J. Serb. Chem. Soc.* **69** (2004) 43
12. R. Walker, S. J. Duncan, *Surf. Technol.* **23** (1984) 301
13. A. Agrawal, S. Kumari, D. Bagchi, V. Kumar, B. D Pandey, *Miner. Eng.* **20** (2007) 95



14. N. D. Nikolić, K. I. Popov, Lj. J. Pavlović, M. G. Pavlović, *Sensors* **7** (2007) 1
15. N. D. Nikolić, G. Branković, M. G. Pavlović, K. I. Popov, *J. Electroanal. Chem.* **621** (2008) 13
16. N. D. Nikolić, Lj. J. Pavlović, S. B. Krstić, M. G. Pavlović, K. I. Popov, *Chem. Eng. Sci.* **63** (2008) 2824
17. N. D. Nikolić, Lj. J. Pavlović, M. G. Pavlović, K. I. Popov, *J. Serb. Chem. Soc.* **72** (2007) 1369
18. N. D. Nikolić, K. I. Popov, Lj. J. Pavlović, M. G. Pavlović, *J. Solid State Electrochem.* **11** (2007) 667.

